Published online November 15, 2018

Journal of Environmental Quality

TECHNICAL REPORTS

SURFACE WATER QUALITY

Tile Drainage as a Hydrologic Pathway for Phosphorus Export from an Agricultural Subwatershed

Aubert R. Michaud, Simon-Claude Poirier, and Joann K. Whalen*

Abstract

Cyanobacteria growth in Missisquoi Bay of Lake Champlain is triggered by the P load carried by tributaries in surrounding watersheds where agriculture is a dominant land use. The objective of this study was to apportion the total P (TP) load in streamflow from an agricultural subwatershed into distinct hydrologic pathways: groundwater resurgence, surface runoff, and tile drainage components (matrix flow and preferential flow). Stream discharge during peak flow was separated into these four components using electrical conductivity (EC)–discharge relationships developed from the stream water EC at the subwatershed outlet and from EC values of surface runoff and tile drain water in 10 fields within the subwatershed. The four-component hydrograph model revealed that 46 to 67% of the TP load at the outlet originated from surface runoff during peak flow. Preferential flow was responsible for most of the particulate P and dissolved reactive P loads lost through tile drainage. Groundwater resurgence was a minor source of TP, whereas other sources such as streambank erosion and resuspended sediments contributed up to 21% of the TP load and from 36 to 41% of the particulate P load at the subwatershed outlet. This work confirms that tile drainage contributes to the TP load in agricultural subwatersheds in the Missisquoi Bay region.

Core Ideas

- Field water sources affected electrolytes and electrical conductivity in streamflow.
- Water yield from field hydrologic pathways was deduced from the stream hydrograph.
- Matrix and preferential flows to tile drainage, and surface runoff, were quantified.
- Preferential flow was an important source of sediment and P loads in streamflow.
- Stream water quality may be negatively affected by tile drainage outflows.

In rural areas, much of the P entering aquatic ecosystems originated from agricultural lands (Smith and Schindler, 2009). Subsurface processes are expected to be an important pathway for water discharge and P transport in the cold, humid temperate regions where agricultural lands are often drained to permit farming activities. Tile drainage accounted for 42 to 60% of annual water discharge from agricultural watersheds in the Great Lakes region of Canada (Culley and Bolton, 1983; Macrae et al., 2007) and represented between 53 and 80% of water discharged from agricultural fields in the Pike River watershed of Quebec, Canada (Gangbazo et al., 1997; Jamieson et al., 2003; Enright and Madramootoo, 2004). In this region, ~40% of the annual total P (TP) loss from agricultural fields occurs through tile drainage (Macrae et al., 2007; Eastman et al., 2010). The TP load contains dissolved P and particulate P (PP) compounds. The concentrations of dissolved P and PP depend on soil properties and hydrologic processes, which exhibit seasonal variation. Dissolved reactive P (DRP) was the dominant P form in tile drainage during winter and spring months, whereas the PP concentration increased in summer (Macrae et al., 2007), possibly due to the presence of soil cracks that acted as preferential flow pathways for PP during the summer (Stamm et al., 1998; Geohring et al., 2001). Tile drainage transports these compounds via two hydrologic pathways, namely matrix flow that moves dissolved P compounds through micropores and preferential flow that transports dissolved P plus PP through macropores to tile drains (Steenhuis et al., 1994).

Apportioning the TP load in agricultural catchments into the dissolved P and PP loads transported via tile drainage and other hydrological pathways (i.e., surface runoff and groundwater resurgence) is necessary to quantify the magnitude of P transfers from agricultural fields and their impact on stream water quality. Electrical conductivity (EC) is correlated with the semiconservative electrolyte concentration in stream water and follows a predictable pattern (Walling and Webb, 1980). The EC of streamflow can differentiate surface runoff from subsurface outflows in hydrograph separation models (Pilgrim et al., 1979;

J. Environ. Qual.
doi:10.2134/jeq2018.03.0104
Supplemental material is available online for this article.
Received 24 Mar. 2018.
Accepted 4 Oct. 2018.
*Corresponding author (joann.whalen@mcgill.ca).

A.R. Michaud and S.-C. Poirier, Institut de recherche et de développement en agroenvironnement, 2700 rue Einstein, Quebec City, QC, Canada G1P 3W8; S.-C. Poirier and J.K. Whalen, Dep. of Natural Resource Sciences, Macdonald Campus, McGill Univ., 21111 Lakeshore Rd., Ste-Anne-de-Bellevue, QC, Canada H9X 3V9.
Assigned to Associate Editor Douglas Smith.

Abbreviations: BAP, bioavailable phosphorus; DRP, dissolved reactive phosphorus; EC, electrical conductivity; L_i, instantaneous load; NSE, Nash–Sutcliffe efficiency; Pbias, percentage of bias; PP, particulate phosphorus; RMSE-RSR, root mean square error/observations standard deviation ratio; TP, total phosphorus; TSS, total suspended solids.

Matsubayashi et al., 1993), and this was confirmed for surface and subsurface discharges in 16 rural watersheds of southern Quebec (Michaud et al., 2009a, 2014). Electrolyte mass balance according to Ca concentration (Chikhaoui et al., 2008), EC, and O^{18}/O^{16} methods (Vidon and Cuadra, 2010) can distinguish the contributions of matrix and preferential flows to tile drainage discharge in agricultural land with contrasting soil texture and cropping systems. In tile-drained agroecosystems, the proportions of dissolved P and PP that move through matrix and preferential flow pathways vary temporally due to climatic factors, primarily rainfall, that affect the integrity of flow pathways and physicochemical interactions between nutrients and the soil matrix (Chikhaoui et al., 2008; Vidon and Cuadra, 2011; Williams et al., 2016). Water and P discharge from agricultural fields derived from hydrograph segmentation and semiconservative tracer methods could be extrapolated to larger spatial and longer temporal scales, but this is seldom done.

The objective of this study was to apportion the TP load in streamflow from an agricultural subwatershed to four distinct hydrologic pathways: groundwater resurgence, surface runoff, and two tile drainage components (matrix flow and preferential flow). Hydrologic pathways in 10 agricultural fields with different soil and crop characteristics were evaluated to represent the agricultural outflows from various land uses in the Ewing Brook subwatershed. Relationships between water discharge and the physicochemical composition of field-collected water samples were then used to deduce the contribution of each hydrologic pathway to the TP, PP, and dissolved P loads at the subwatershed outlet.

Materials and Methods

Study Area

The Ewing Brook subwatershed (32.2 km^2), hereafter referred to as the Ewing subwatershed, is located within the Pike River watershed in southern Quebec, Canada (Fig. 1). This cold, humid, temperate region has monthly air temperature from −10.0°C in January to 20.5°C in July, and precipitation falls as rain (932 mm yr^{-1}) or snow (200 mm yr^{-1}; Government of Canada, 2018). The Ewing subwatershed is flat (mean slope < 1%), and surface soils are sandy Spodosols to clayey Inceptisols overlying poorly drained clay subsoils of marine and lacustrine origin (Michaud et al., 2009b). Agriculture accounts for 98% of the land use and is dominated by annual corn (*Zea mays* L.) production on sandy soils (47% of fields) and clayey soils (32% of fields) grown in rotation with soybean [*Glycine max* (L.) Merr.] and small grains (8% of annual land use), whereas hayfields with perennial forages occupy 13% of land use in the subwatershed (Fig. 1).

Water Sample Collection and Analysis

Experimental fields were upstream on first-order stream branches and the subwatershed outlet gauge was downstream on the third-order stream branch. Fields included five sandy loam soils and three clay loam soils under corn production (i.e., annual crop) plus two clay loam soils under hay production (i.e., perennial crop). Tile drainage area was assumed to coincide with the surface runoff contributing area in each field, according to a numerical elevation model derived from 1.0-m-resolution LiDAR (light detection and ranging) data (Michaud et al., 2009b). Sample collection, analysis, and water quality of surface runoff and tile drainage were described by Poirier et al. (2012). Streamflow discharge and precipitation at each sampling date are summarized in Supplemental Fig. S1. Briefly, water was collected manually from tile drain outlets on 19 sampling dates from 1 Oct. 2008 to 31 May 2009 when peak flows occurred at the watershed outlet (10 times in fall and nine times in spring). Surface runoff was collected manually from the field ditch outlet, when available, on nine sampling dates (five times in fall and four times in spring). Water samples were stored in high-density polyethylene bottles at 4°C and analyzed within 3 wk for total suspended solids (TSS) collected on a 0.45-μm filter (Method # 2540D; APHA, 2005). In addition, P concentrations were quantified colorimetrically with the molybdenum blue method (Murphy and Riley, 1962) for DRP in water filtered to <0.45 μm, bioavailable P (BAP) in 0.1 M NaOH extracts (Sharpley et al., 1991), dissolved total P in water filtered to <0.45 μm, and TP in unfiltered water by the persulfate digestion technique (Method no. 4500-P-B; APHA, 2005). Particulate P (PP, in mg L^{-1}) was the difference between TP and dissolved total P. The NO_3–N concentration was analyzed by Method no. 4500-NO_3–F (APHA, 2005), pH and EC were measured, and dissolved Ca, Mg, K, and Na concentrations were determined in water filtered to <0.45 μm by inductively coupled Ar plasma emission spectrometry.

Stream Monitoring

Water height was measured automatically every 15 min with a bubbler (Alphée 3010, Hydrologic-H2I) installed near the Ewing subwatershed outlet. The stage–discharge relationship was determined by seasonal and peak flow rate measurements with a current propeller. A multiparameter probe (YSI 600XL, YSI) provided measurements every 15 min of stream water temperature, turbidity, and EC. Stream water was collected manually within 3 h of field water sampling (n = 19) and two to three more times during peak flow (n = 51) on the rising and recession limbs of the hydrograph and analyzed for TSS, pH, EC, and the nutrients described above.

Sediment and nutrient content in stream water samples were expressed as the instantaneous load (L_i, in g min^{-1}), the product of the streamflow discharge (mm d^{-1}, equivalent to 6.94×10^{-7} m min^{-1}) and the sediment or nutrient concentration (mg L^{-1}, expressed as g m^{-3}), multiplied by the subwatershed area (3220 ha = 3.22×10^7 m^2). Sediment and nutrient loads (g ha^{-1}) exported in stream water during each season (fall 2008 and spring 2009) were the sum of each L_i multiplied by the time (min) between sampling events, divided by the subwatershed area (3220 ha). The L_i–discharge relationship was described with polynomial square root or logarithmic relationships after analysis of covariance using JMP 8.0 (SAS Institute, 2008).

Four-Component Hydrograph Model for the Ewing Subwatershed

The four-component hydrograph model relied on continuous EC monitoring of stream water, coupled with discrete EC measurements, to apportion streamflow into four distinct hydrologic pathways: groundwater resurgence, surface runoff, and tile drainage components (matrix flow and preferential flow). Groundwater resurgence generated a base flow with EC from 0.50 (Fig. 2) to 0.75 mS cm^{-1}. Resurgence flow end member during peak flow

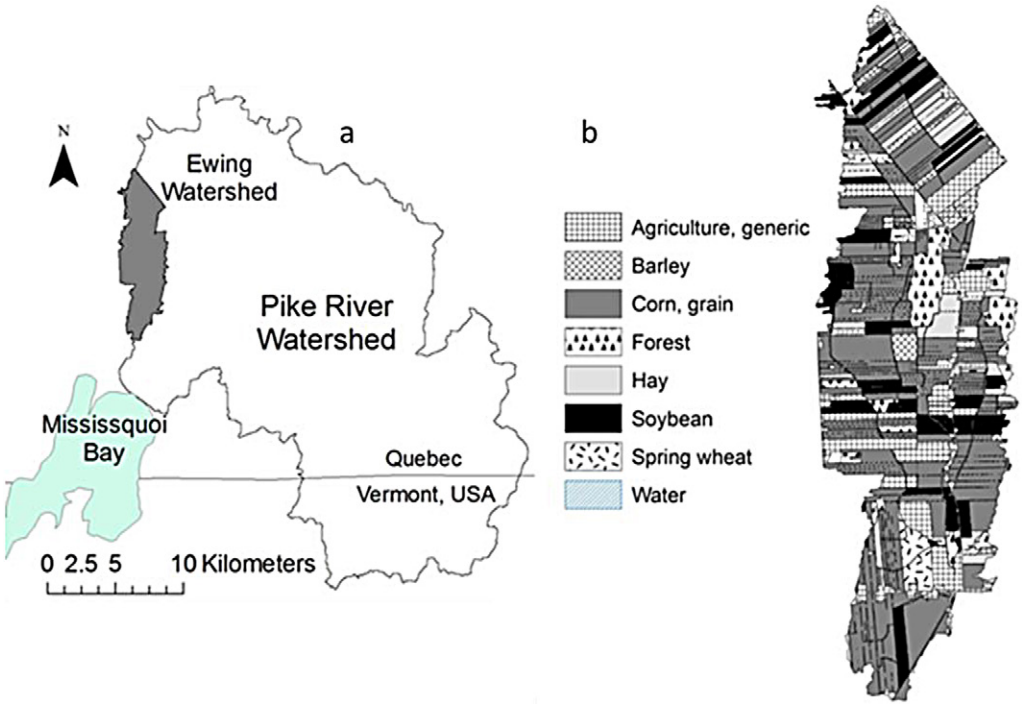

Fig. 1. (a) Map of Ewing subwatershed of the Pike River watershed showing (b) the land use in 2008, as reported by La Financière Agricole du Québec (2009).

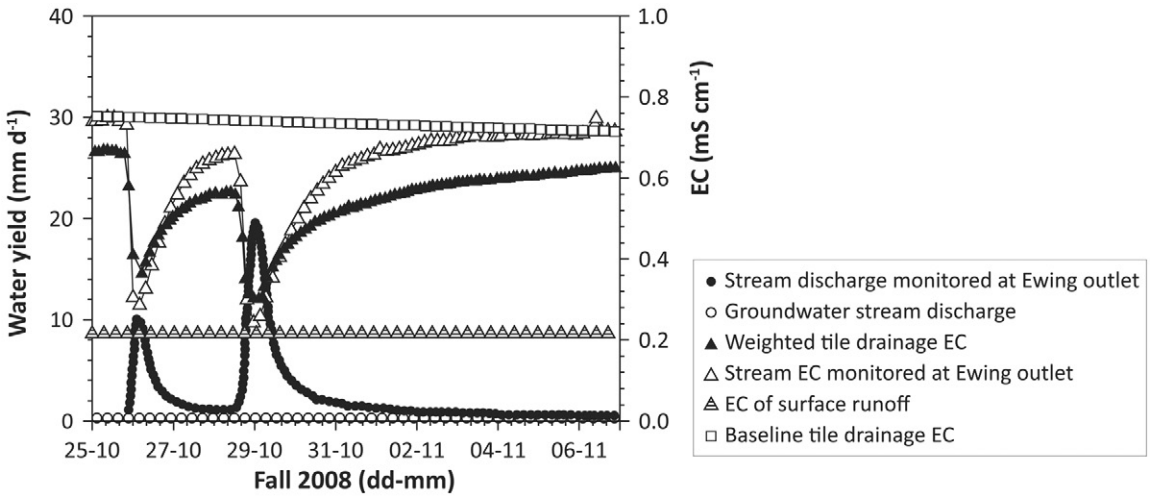

Fig. 2. Conceptual model of the four-component hydrograph model that accounts for groundwater resurgence, surface runoff, and two subsurface pathways (matrix flow and preferential flow) associated with tile drainage. Stream discharge (●) and electrical conductivity (EC, △) measured at the Ewing subwatershed outlet every 15 min were assumed to be a function of the volume and EC of each water source. In this example, surface runoff had EC of 0.22 mS cm^{-1}. Water from tile drains had relatively high EC, reflecting the input of electrolyte-rich water that passed through the soil matrix plus water transported through soil macropores, a preferential flow pathway. Baseline tile drainage (□) reflects the high proportion of matrix water in tile drainage, expressed as a linear relationship between the EC maximum measured at the Ewing subwatershed outlet prior to the onset of surface runoff and the EC at the end of the event. Weighted tile drainage (▲) was estimated from the average EC measured in tile drainage at field sites and extrapolated to the area under three major land uses (annual crops on sandy soil, annual crops on clayey soil, and hayfields) in the subwatershed.

events was determined from the linear relationship between the initial stream flow rate, which represented maximum EC prior to initiation of the rising limb, and the final flow rate when EC returned to the pre-event level, after completion of the recession limb (Fig. 2.). Changes in stream water EC during a peak flow event were attributed to the volume and EC of water entering the stream from fields via surface runoff and tile drainage pathways (Fig. 2). Surface runoff EC was the average EC of surface runoff collected from field sites (0.22 ± 0.08 mS cm^{-1}), which did not differ significantly among sites or sampling events ($p > 0.05$, data not shown). Tile drainage had higher EC than surface runoff due to longer contact time with electrolyte-rich soil. For each event, two calculations were applied to express the EC of tile drainage water: (i) a calculation based on the stream EC signal, and (ii) a calculation based on field water EC, upscaled at the subwatershed scale. For each event, the baseline EC of tile drainage was derived from the linear relationship between the highest EC measured in streamflow, prior to the onset of surface runoff, and the EC measured in streamflow at the end of the event (Fig. 2). Conceptually, the stream baseline method assumes that the EC of tile drainage water remains elevated throughout the event (Fig. 2), suggesting a relatively slow, matricial flow path.

The weighted EC of tile drainage shown in Fig. 2 is an EC–discharge relationship that captures the significant intra-event variability of EC in tile drainage at field outlets (data not shown). This assumed that EC from individual fields was representative of the EC in water outflows from three land uses (annual crop on sandy soil, annual crop on clayey soil, and hayfield) in the Ewing subwatershed. Conceptually, the lower EC signal derived from field-weighted data, compared with the stream baseline method (Fig. 2), was attributed to the mixing of water from preferential flow (low EC) and matricial flow (elevated EC). Subsurface (drainage) flow at time i (QD_i, in mm d^{-1}) in the stream was estimated from the stream baseline and field weighted EC values using Eq. [1]:

$$QD_i\left(\frac{EC_i - EC_S}{EC_{TD,i} - EC_S}\right)Q_{peak,i} \quad [1]$$

where EC_i is the measured EC in streamflow at time i, EC_S is the average EC of 0.22 mS cm^{-1} in surface runoff water, $EC_{TD,i}$ is the estimated EC of the streamflow contribution from tile drainage (either the stream baseline EC or field-weighted EC) at time i, and $Q_{peak,i}$ represents the peak water discharge (mm d^{-1}) at time i, after subtracting the contribution of groundwater resurgence to discharge. Assuming that drain water yield (QD_i) estimated from stream baseline EC values represents water transported via matrix flow to tile drains, consequently, preferential flow was the difference between tile drainage (field weighted method) and matricial flow (stream baseline method).

Hydrograph separation, together with the measured sediment and nutrient concentrations in field water and at the outlet, was used to predict the instantaneous load (L_i in g min^{-1}) of sediments and nutrients from four hydrological pathways. The mass balance equation used to predict L_i (Eq. [2]) accounted for water yield and sediment and nutrient transport from each pathway under three land uses (annual crop on sandy soil, annual crop on clayey soil, and hayfields):

$$\text{Predicted } L_i = \frac{\begin{pmatrix} Q_{Gr\_i}C_{Gr\_i} + A_iQ_{Sr\_i}C_{Sr\_i} \\ + A_iQ_{TD\_i}C_{TD\_i} \end{pmatrix}A_{SUB}}{K} \quad [2]$$

All values are calculated or measured at time i, where Q_{Gr_i} is the groundwater resurgence discharge (mm d^{-1}), C_{Gr_i} is the sediment or nutrient concentration of groundwater (g L^{-1}) derived from the L_i–discharge relationship, Q_{SR_i} is the surface runoff water yield (mm d^{-1}) estimated from L_i–discharge relationships, C_{SR-i} is the sediment or nutrient concentration measured in the field ditch (g L^{-1}), Q_{TD_i} is the tile drainage water yield (mm d^{-1}) estimated from L_i–discharge relationships, and C_{TD-i} is the sediment or nutrient concentration measured in field tile drainage (g L^{-1}). A_j represents the proportion of subwatershed area under each land use, namely 0.51 for annual crop on sandy soil, 0.36 for annual crop on clayey soil, and 0.13 for hayfield. Total subwatershed area (A_{SUB}, 3.22×10^7 m^2) and the constant (K, 1440 min d^{-1}) are included to balance the equation.

Statistical Analysis

Predicted L_i values were compared to observed nutrient loads with the model evaluation criteria proposed by Moriasi et al. (2007): the Nash–Sutcliffe efficiency (NSE), the percentage of bias (Pbias), and the root mean square error/observations standard deviation ratio (RMSE-RSR) to evaluate the goodness of fit of modeled values.

Results

Electrical Conductivity in Streamflow Is an Indicator of Water Sources from Fields

Electrical conductivity at the Ewing subwatershed outlet was positively correlated with the Ca, Mg, and Na concentrations ($r > 0.90$, $p \leq 0.01$) and pH ($r = 0.74$, $p \leq 0.01$) but negatively correlated with the K concentration ($r = -0.34$, $p \leq 0.01$) and TSS ($r = -0.74$, $p \leq 0.01$) of stream water (Supplemental Table S1). Surface runoff from fields had a mean (± SE) Ca concentration of 28 (± 7) mg Ca L^{-1} and an EC of 0.22 (± 0.08) mS cm^{-1}. Tile drainage EC depended on the water movement through matrix flow and preferential flow pathways. For instance, the highest Ca concentration and EC at the end of the recession limb was attributed to the matrix flow component, since EC in these samples was positively correlated ($p < 0.05$) with the EC in subsoil samples (70- to 90-cm depth) but not topsoil (0- to 20-cm depth, data not shown). The lowest EC in tile drainage was measured close to the peak of the rising limb and coincided with the highest TSS and TP concentrations in tile drainage, which were presumably transported via preferential flow, and had low EC due to short contact time with the Ca-rich subsoil. For simplicity, we assumed no subsurface water mixing through fingering, funnel, lateral and heterogeneous processes that contribute to preferential flow (Jarvis, 2007). These results confirm that EC is a suitable indicator of water sources that contribute to streamflow in the Ewing Brook.

Water Yield Estimated by the Four-Component Hydrograph Model

Discharge at the Ewing subwatershed outlet was 0.3 to 19.6 mm d^{-1} during fall 2008 and 0.2 to 9.0 mm d^{-1} in spring 2009. Groundwater resurgence represented 41 (fall 2008) to 50% (spring 2009) of total water yield at the outlet (Table 1). Surface runoff was 10 to 11% of the total water yield in fall and spring, according to the field weighted method, and contributed less to water yield than tile drainage (Table 1). Total tile drainage was 40 to 48% of the total water yield, depending on season, primarily through matrix flow (Table 1).

Nutrient Loads in Relation to Water Yield at the Ewing Subwatershed Outlet

The L_i of TSS and nutrient concentrations (Ca, NO_3–N, and P pools) at the Ewing subwatershed outlet increased, whereas the EC in streamflow declined, as the water yield increased (Fig. 3). Best-fit lines are shown for the measurement period (TSS, EC, Ca, NO_3–N, and PP concentrations) or by season, due to significantly ($p < 0.05$) lower TP, BAP, and DRP concentrations in spring 2009 than in fall 2008 (Fig. 3). Power relationships, indicating gradual decline to a minimum or gradual increase to

Table 1. Water yields from groundwater resurgence (GR), surface runoff (SR), total tile drainage (TD), and tile drainage through preferential flow only (TD-PF). Total water yield at the Ewing subwatershed outlet during the measurement periods (fall 2008 and spring 2009) was partitioned with a four-component hydrograph model using the baseline tile drainage and weighted tile drainage methods. Model estimates are the means (± SE) associated with each water source.

Season	Water yield							
	Total	Field-weighted method				Stream baseline method		
		GR	SR	TD	TD-PF†	GR	SR	TD
	mm	mm (%)			mm (%, %)	mm (%)		
Fall 2008	67 ± 0.3	28 ± 0.2 (41)‡	7.0 ± 0.2 (11)	32 ± 0.2 (48)	14 ± 0.2 (21‡, 44§)	28 ± 0.2 (41)	21 ± 0.2 (31)	18 ± 0.2 (27)
Spring 2009	116 ± 0.3	58 ± 0.3 (50)	12 ± 0.2 (10)	46 ± 0.2 (40)	14 ± 0.2 (13‡, 30§)	58 ± 0.3 (50)	26 ± 0.2 (23)	32 ± 0.2 (27)

† Calculated, the difference between baseline tile drainage and weighted tile drainage.

‡ Percentage of total water yield at the subwatershed outlet.

§ Percentage of the total water yield from tile drainage.

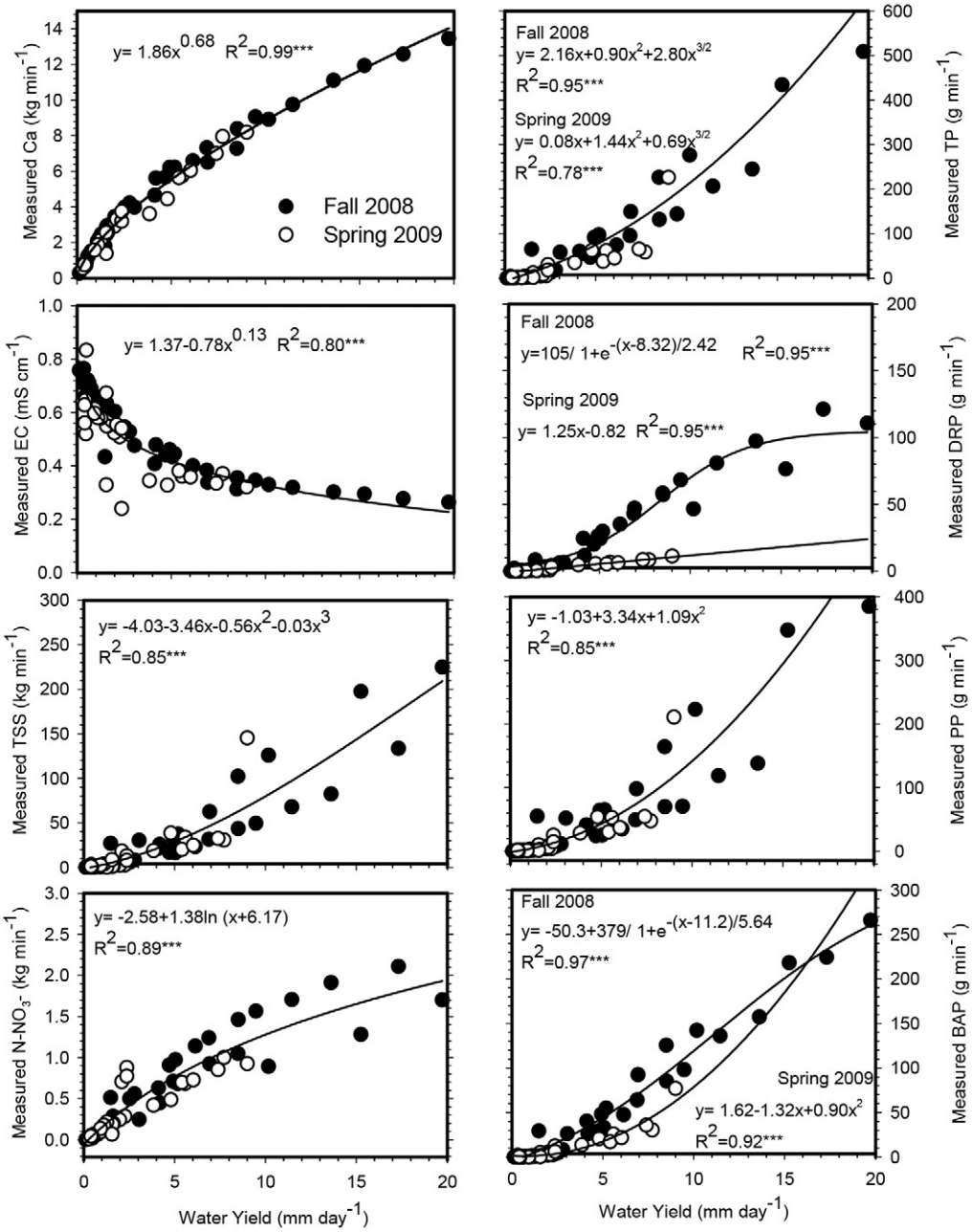

Fig. 3. Electrical conductivity (EC) and instantaneous loads of nutrients and sediments measured at Ewing subwatershed outlet, in relation to water yield. Data points are from fall 2008 (●) and spring 2009 (○) sampling events (n = 70). Equations of the line represent the curve used to estimate loads for the given period. * Significant at $p \leq 0.001$. Abbreviations: TSS, total suspended solids; TP, total P; PP, particulate P; DRP, dissolved reactive P; BAP, bioavailable P.**

a maximum, described the response of EC and Ca and NO_3–N concentrations to increasing water yield (Fig. 3). In contrast, the TSS and the P pools (TP, PP, BAP, and DRP concentrations) showed quadratic or exponential increases with higher water yields, which suggests that sediment and P loads will increase dramatically beyond a threshold water yield of ~5 to 10 mm d^{-1} (estimated from Fig. 3). Sediment and nutrient loads showed consistent relationships with water yield in both seasons, although the DRP load followed a sigmoidal curve in fall 2008 and a linear relationship in spring 2009 (Fig. 3).

Nutrient Loads Partitioned among Water Sources with the Four-Component Hydrograph Model

Predicted EC and predicted Ca and NO_3–N loads at the Ewing subwatershed outlet corresponded well with observed values, and most points were on the 1:1 line (Fig. 4) with NSE coefficients of 0.86 to 0.91, RMSE-RSR of 0.31 to 0.37, and Pbias of −7.0 to 5.2% (Supplemental Table S2). Loads of TSS, TP, and PP tended to be underestimated by the four-component hydrograph model, whereas the DRP was overestimated and the BAP fit on the 1:1 line (Fig. 4). More uncertainty was associated with the predicted TSS, PP, and DRP loads, which had NSE of 0.42 to 0.69, RMSE-RSR values as high as 0.76, and greater deviation from 0 in the Pbias (−18 to 46%, Supplemental Table S2) than the predicted TP and BAP loads, although the Pbias indicated deviation of 24 to 34% between predicted and observed TP and BAP loads (Supplemental Table S2).

Relationships between observed values at the Ewing subwatershed outlet and predicted values from the four-component hydrograph model (Fig. 4) indicate that the predicted Ca load generally fit the 1:1 line with NSE = 0.92, RMSE-RSR = 0.29, and Pbias = −2.6% (Supplemental Fig. S2). Greater variability was expected for the predicted TP load, according to Fig. 4, but there was a relatively good fit with the 1:1 line with NSE = 0.69, RMSE-RSR = 0.56, and Pbias = 31% (Supplemental Fig. S2). Consequently, the four-component hydrograph model was constrained by a factor called "other sources" (Tables 2 and 3) to correct the discrepancy between observed and predicted loads of TSS and P pools in streamflow.

Groundwater resurgence was the source of up to 62% of the Ca load and as much as 45% of NO_3–N load, whereas tile drainage accounted for 38 to 43% of the Ca load and 54 to 58% of the NO_3–N load (Table 2). Less than 5% of the Ca and NO_3–N loads came from surface runoff (Table 2). Matricial flow contributed more to the Ca and NO_3–N loads than preferential flow (Table 2). Predicted Ca and NO_3–N loads were the same as the estimated Ca and NO_3–N loads, with ≤3% deviation between predictions from four-component hydrograph model and loads estimated from the L_i–discharge relationship (Table 2).

Predicted loads of TSS and P pools from the four-component model differed from the loads estimated with the L_i–discharge relationship, owing to the contribution of "other sources." For example, ~43% of the TSS load and 36 to 41% of the PP load (Table 3) came from other sources, which implies that these materials were already in the stream and arrived at the outlet during the measurement period. Tile drainage contributed to loading of TSS and P pools (Table 3), mostly through the preferential flow pathway, which transported ≥85% of the drainage-associated TSS and P pools in fall 2008, and ≥70% of the drainage-associated TSS, TP, and PP loads in spring 2009 (Table 3).

Discussion

Streamflow EC was associated with mobile electrolytes like Ca, Mg, and Na, consistent with the positive relationship between EC and Ca and Mg concentrations in tile drainage from annually cropped fields in the Pike River watershed (Chikhaoui et al., 2008). As Ca, Mg, and Na concentrations were negatively correlated with TSS, they were probably not released from suspended sediments in the streamflow. Therefore, EC could differentiate water with a high concentration of dissolved electrolytes, such as groundwater resurgence (Pilgrim et al., 1979) and subsurface matricial flow, from water with a lower concentration of dissolved electrolytes like surface runoff and the preferential flow component of tile drainage (Chikhaoui et al., 2008; Vidon and Cuadra, 2010).

Precipitation affects water yield in Ewing Brook and was lower in fall 2008 when less precipitation (<50 mm mo^{-1}) occurred. Stream discharge was 15% of total precipitation in fall 2008 and 29% of the precipitation during spring 2009, consistent with the discharge of 25 to 37% of total precipitation from nonfrozen soils in the Pike River watershed (Michaud et al., 2009a). Most of the water yield from agricultural fields came from tile drainage, and the tile drainage/surface runoff ratio was 0.79 to 0.82 according to the stream baseline method, which is similar to the tile drainage/surface runoff ratio of 0.73 to 0.84 in annually cropped fields with sandy and clayey soils (Eastman et al., 2010). Preferential flow represented 30 to 44% of the total tile drainage in this study. This range is narrower than in another study from the same agroclimatic region, where Chikhaoui et al. (2008) reported that preferential flow was 20 to 70% of total tile drainage, depending on topsoil texture and macroporosity. Our approach, which aggregated data to make estimates of flow pathways in an agricultural subwatershed on a seasonal basis, cannot capture the fine-scale hydrologic processes occurring in tile drainage at the field scale and between or within sampling events that are reported elsewhere (Vidon and Cuadra, 2011; Williams et al., 2016). The preferential flow contribution to tile drainage remains difficult to quantify because it is influenced by rainfall amount and intensity (Edwards et al., 1993), antecedent soil moisture (Edwards et al., 1993; Weiler and Naef, 2003), the activity of soil macrofauna, and field management (Jarvis, 2007).

Preferential flow was a minor source of dissolved nutrients (e.g., Ca, NO_3–N, and DRP) transported through tile drainage but was responsible for ≥70% of the TSS, TP, and PP lost through tile drainage on a seasonal basis. The disproportionate amount of sediment and sediment-associated nutrients lost through preferential flow could be coming from detached particles at the soil surface, which enter macropores connected to tile drainage. Subsurface erosion within the soil profile is another possibility, given that Klaus et al. (2013) observed preferential flow water originating from the soil matrix at a depth of 20 to 40 cm, after a soil water storage threshold was exceeded, but this remains to be confirmed.

Observed EC and Ca and NO_3–N loads corresponded to predicted values from the four-component hydrograph model, according to the model evaluation criteria of Moriasi et al. (2007). We considered Ca to be a semiconservative tracer of water sources according to the mass balance concept of Genereux (1998),

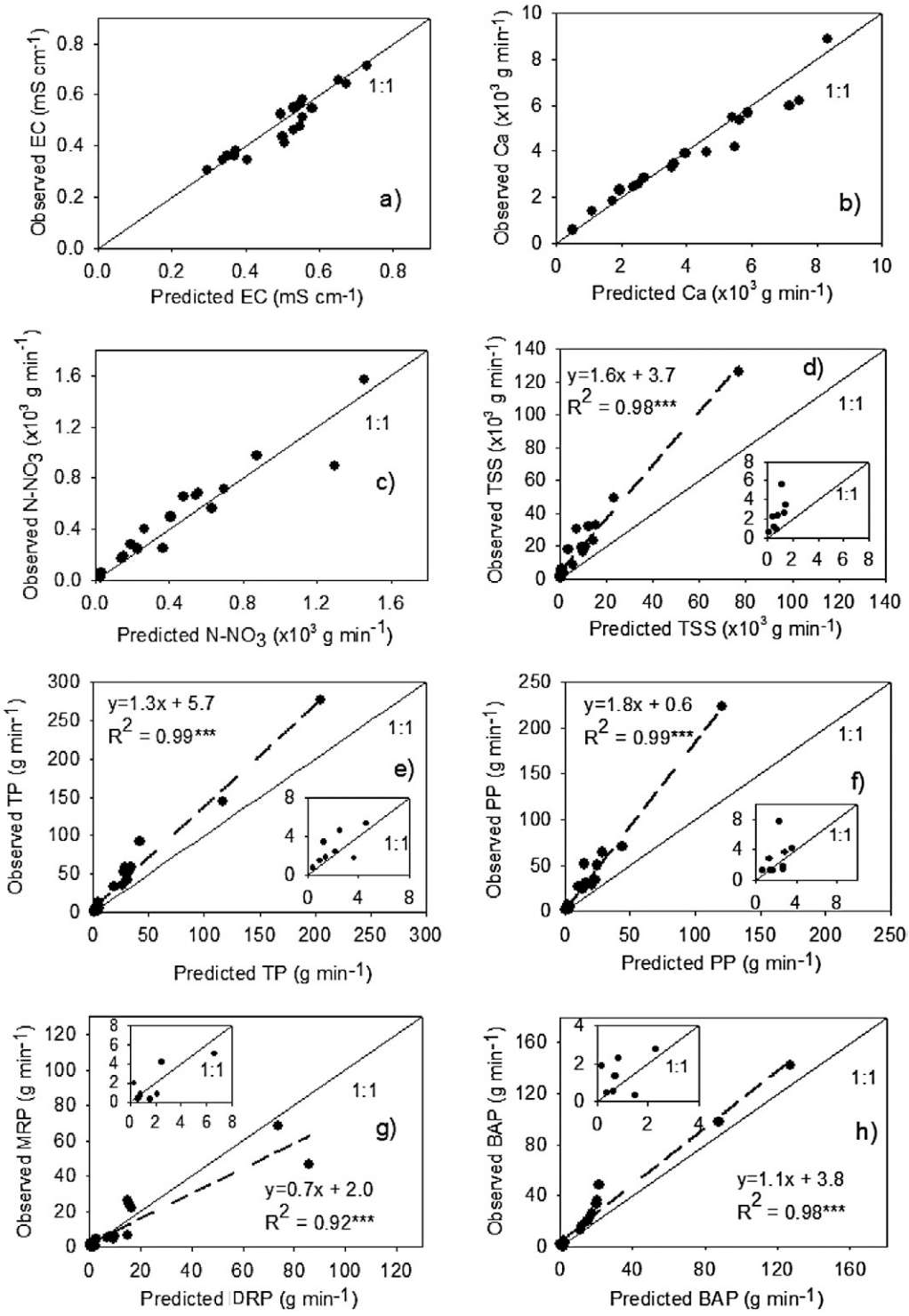

Fig. 4. Relationship between observed (*n* = 19) and predicted values for electrical conductivity (EC) and instantaneous loads of sediment and nutrients at the Ewing subwatershed outlet. Predicted values were from the four-component hydrograph separation model, developed from stream hydrographs and the field-scale measurements of sediment and nutrient concentrations. Equations of the lines were significant at $p \leq 0.001$, indicated as *. Abbreviations: TSS, total suspended solids; TP, total P; PP, particulate P; DRP, dissolved reactive P; BAP, bioavailable P.**

whereas NO_3–N was a tracer of mobile nutrient loss from agricultural fields through subsurface drainage primarily, rather than surface runoff, due to the ease with which NO_3–N moves through matrix flow and its sensitivity to cropping practices and N fertilizer management (Hatch et al., 2002; David et al., 2010).

The four-component hydrograph model was less accurate in predicting loads of TSS and P pools, according to the goodness of fit (1:1 line), NSE, RMSE-RSR, and Pbias statistics. This was not surprising, since we assumed conservative transport of TSS and P pools and did not account for processes occurring in the stream phase, such as streambank erosion and adsorption, which we term "other sources." Since TSS from fields (e.g., in surface runoff and tile drainage) were generally <100 μm with a bimodal distribution that peaked at 0.45 and 5 μm (Poirier et al., 2012), we expect them to remain suspended in streamflow. However, we cannot rule out the possibility that TSS from fields underwent aggregation

and sedimentation upon entering the stream. We also made assumptions about the TSS load from groundwater resurgence, which need to be confirmed with in-stream measurements. As the observed TSS load was greater than the predicted TSS load, another source of sediments must have entered the stream between the field and the outlet. These sediments may originate from streambank erosion, which accounted for 29% of TSS in an agricultural watershed in southern Ontario (Knap and Mildner, 1978) or may be resuspended in the stream channel. About 40% of the PP load came from "other sources." Again, streambank and resuspended sediments may contribute to the PP load; another possibility is that the PP load was enriched by physical sorting of particles along the transfer path between field ditches and the outlet. We do not know how much suspended PP from fields was sedimented and resuspended within an event, or between events, as we lack the requisite data (e.g., ^{137}Cs) to trace these physical processes.

Accounting for seasonal variation in hydrologic processes, our study confirmed the importance of surface runoff and revealed that preferential flow was responsible for transporting TSS, TP, PP, and DRP from tile drained fields of an agricultural subwatershed into the Ewing Brook. This suggests that preferential flow is relatively enriched with P-rich sediments that may have infiltrated soil macropores and entered tile drainage without passing through the matrix, a classic example of bypass flow, although other explanations are possible. In our agroclimatic region, surface water protection strategies that focus exclusively on controlling surface runoff will not succeed in preventing P losses from tile-drained fields. Consideration must be given to the P lost through tile drains when assessing or planning management practices to reduce agricultural nonpoint-source P exported to streams, particularly in agricultural watersheds where extensive subsurface drainage systems are present.

Supplemental Material

Supplemental Table S1 shows correlations between chemical and physicochemical parameters in water samples at the Ewing subwatershed outlet. Supplemental Table S2 gives the model

Table 2. Predicted loads of Ca and NO_3–N at the Ewing subwatershed outlet (estimated load) in fall 2008 and spring 2009. The four-component hydrograph model was used to partition the load from water sources, including groundwater resurgence (GR), surface runoff (SR), total tile drainage (TD), and other sources. The load coming from the matrix flow (TD-Matrix) and the preferential flow (TD-PF) components of tile drainage were calculated with the hydrograph model. The proportion of preferential flow in the total tile drainage is presented as the TD-PF/TD ratio.

Load and season	GR	SR	TD	Other sources†	Estimated load‡	TD-Matrix§	TD-PF¶	TD-PF/TD
				$\times 10^3$ g ha^{-1} (%)				
Ca								
Fall 2008	32 ± 0.1 (62)#	1.0 ± 0.02 (2)	20 ± 0.1 (38)	−1.1 ± 0.1 (−2)	51 ± 0.03	12 ± 0.2 (23)	7.6 ± 0.2 (14)	0.39
Spring 2009	36 ± 0.1 (56)	3.8 ± 0.4 (4)	28 ± 0.1 (43)	−3.2 ± 0.4 (−3)	65 ± 0.04	19 ± 0.1 (29)	9.0 ± 0.1 (14)	0.32
NO_3–N								
Fall 2008	1.9 ± 0.1 (45)	0.10 ± 0.002 (3)	2.3 ± 0.01 (54)	−0.1 ± 0.1 (−2)	4.3 ± 0.2	1.3 ± 0.005 (31)	1.0 ± 0.01 (23)	0.43
Spring 2009	2.2 ± 0.01 (39)	0.20 ± 0.005 (3)	3.3 ± 0.02 (58)	0.0 ± 0.02 (0)	5.8 ± 0.02	2.2 ± 0.01 (40)	1.0 ± 0.02 (18)	0.31

† Calculated, the difference between observed loads in Fig. 4 and the predicted load from the four-component hydrograph model.

‡ Estimated load, based on the observed instantaneous load–discharge relationship.

§ Calculated, the difference in the load from TD and TD-PF.

¶ Calculated, the difference in the load from baseline tile drainage and weighted tile drainage.

Percentage of total load (estimated) at the subwatershed outlet.

Table 3. Predicted loads of total suspended solids (TSS), total P (TP), particulate P (PP), and dissolved reactive P (DRP) at the Ewing subwatershed outlet (estimated load) in fall 2008 and spring 2009. The four-component hydrograph model was used to partition the load from water sources, including groundwater resurgence (GR), surface runoff (SR), total tile drainage (TD), and other sources. The load coming from the matrix flow (TD-Matrix) and the preferential flow (TD-PF) components of tile drainage were calculated with the hydrograph model. The proportion of preferential flow in the total tile drainage is presented as the TD-PF/TD ratio.

Load and season	GR	SR	TD	Other sources†	Estimated load‡	TD-Matrix§	TD-PF¶	TD-PF/TD
TSS, $\times 10^3$ g ha^{-1} (%)								
Fall 2008	22 ± 0.1 (18)#	24 ± 6 (19)	23 ± 1 (19)	53 ± 6 (43)	122 ± 1	3 ± 1 (2)	20 ± 1 (17)	0.87
Spring 2009	26 ± 0.5 (17)	33 ± 4 (22)	27 ± 1 (18)	65 ± 4 (43)	151 ± 1	8 ± 1 (5)	19 ± 1 (13)	0.70
TP, g ha^{-1} (%)								
Fall 2008	24 ± 0.1 (9)	185 ± 24 (67)	74 ± 4 (27)	−7.1 ± 24 (−3)	276 ± 3	9 ± 5 (2)	65 ± 6 (25)	0.88
Spring 2009	13 ± 2 (4)	135 ± 13 (46)	86 ± 1 (29)	60 ± 13 (21)	294 ± 2	22 ± 1 (6)	64 ± 1 (23)	0.75
PP, g ha^{-1} (%)								
Fall 2008	17 ± 0.1 (9)	64 ± 12 (34)	40 ± 1 (21)	67 ± 12 (36)	187 ± 3	5.6 ± 1 (3)	34 ± 1 (18)	0.86
Spring 2009	20 ± 0.1 (3)	61 ± 6 (29)	46 ± 1 (21)	87 ± 6 (41)	215 ± 2	13 ± 1 (6)	33 ± 1 (15)	0.72
DRP, g ha^{-1} (%)								
Fall 2008	4.8 ± 0.1 (6)	40 ± 13 (51)	34 ± 1 (43)	−1.4 ± 13 (−2)	77 ± 1	5 ± 1 (6)	29 ± 1 (38)	0.85
Spring 2009	4.4 ± 0.4 (14)	17 ± 0.1 (40)	23 ± 0.9 (46)	−16 ± 1 (−22)	28 ± 1	13 ± 2 (28)	10 ± 2 (22)	0.43

† Calculated, the difference between observed loads in Fig. 4 and the predicted load from the four-component hydrograph model.

‡ Estimated load, based on instantaneous load –discharge relationship.

§ Calculated, the difference in the load from TD and TD-PF.

¶ Calculated, the difference in the load from baseline tile drainage and weighted tile drainage.

Percentage of total load (estimated) at the subwatershed outlet.

evaluation criteria for EC and nutrient loads (L_i) predicted by the four-component hydrograph model. Supplemental Fig. S1 shows the discharge from the Ewing subwatershed, precipitation, and timing of discrete water sampling during the study. Supplemental Fig. S2 describes the error of predicted loads in the four-component hydrograph model.

Acknowledgments

Thank you to the farmers and stakeholders who provided access to their fields, and to Jacques Desjardins, Charles Lussier, and Richard Lauzier for assistance with the field work. Financial support was from the Partnership Program on Cyanobacteria of the Fonds de recherch sur la nature et les technologies du Quebec. S.-C. Poirier received a postgraduate scholarship from the Natural Sciences and Engineering Research Council of Canada. We thank Dr. Douglas Smith for editorial corrections and three anonymous reviewers for helpful comments on an earlier version of this manuscript.

References

APHA. 2005. Standard methods for examination of waste and waste water. 21st ed. Am. Public Health Assoc., Washington, DC.

Chikhaoui, M., C.A. Madramootoo, M. Eastman, and A.R. Michaud. 2008. Estimating preferential flow to agricultural tile drains. In: Proceedings of the ASABE Annual International Meeting, Providence, RI. 29 June–2 July 2008. Am. Soc. Agric. Biol. Eng., St. Joseph, MI. Paper 083970. doi:10.13031/2013.24812

Culley, J.L.B., and E.F. Bolton. 1983. Suspended solids and phosphorus loads from a clay soil: II. Watershed study. J. Environ. Qual. 12:498–503. doi:10.2134/jeq1983.00472425001200040012x

David, M.B., L.E. Drinkwater, and G.F. McIsaac. 2010. Sources of nitrate yields in the Mississippi River basin. J. Environ. Qual. 39:1657–1667. doi:10.2134/jeq2010.0115

Eastman, M., A. Gollamudi, N. Stämpfli, C.A. Madramootoo, and A. Sarangi. 2010. Comparative evaluation of phosphorus losses from subsurface and naturally drained agricultural fields in the Pike River watershed of Quebec, Canada. Agric. Water Manage. 97:596–604. doi:10.1016/j.agwat.2009.11.010

Edwards, W.M., M.J. Shipitalo, L.B. Owens, and W.A. Dick. 1993. Factors affecting preferential flow of water and atrazine through earthworm burrows under continuous no-till corn. J. Environ. Qual. 22:453–457. doi:10.2134/jeq1993.00472425002200030008x

Enright, P., and C.A. Madramootoo. 2004. Phosphorus losses in surface runoff and subsurface drainage waters on two agricultural fields in Quebec. In: R.A. Cooke, editor, Proceedings of the 8th International Drainage Symposium, St. Joseph, MI. 21–24 Mar. 2004. Am. Soc. Agric. Biol. Eng., St. Joseph, MI. p. 160–170. doi:10.13031/2013.15722

Gangbazo, G., A.R. Pesant, D. Côté, G.M. Barnett, and D. Cluis. 1997. Spring runoff and drainage N and P losses from hog-manured corn. J. Am. Water Resour. Assoc. 33:405–411. doi:10.1111/j.1752-1688.1997.tb03519.x

Genereux, D. 1998. Quantifying uncertainty in tracer-based hydrograph separations. Water Resour. Res. 34:915–919. doi:10.1029/98WR00010

Geohring, L.D., O.V. McHugh, M.T. Walter, T.S. Steenhuis, M.S. Akhtar, and M.F. Walter. 2001. Phosphorus transport into subsurface drains by macropores after manure applications: Implications for best manure management practices. Soil Sci. 166:896–909. doi:10.1097/00010694-200112000-00004

Government of Canada. 2018. Canadian climate normals 1981-2010 station data for Farnham, Quebec. Gov. Canada, Ottawa, ON. http://climate.weather.gc.ca/climate_normals/results_1981_2010_e.html?stnID=5358 (accessed 31 Oct. 2018).

Hatch, D., K. Goulding, and D. Murphy. 2002. Nitrogen. In: P.M. Haygarth and S.C. Jarvis, editors, Agriculture, hydrology and water quality. CAB Int., Wallingford, UK. p. 7–27. doi:10.1079/9780851995458.0007

Jamieson, A., C.A. Madramootoo, and P. Enright. 2003. Phosphorus losses in surface and subsurface runoff from a snowmelt event on an agricultural field in Quebec. Can. Biosyst. Eng. 45:1.1–1.7.

Jarvis, N.J. 2007. A review of non-equilibrium water flow and solute transport in soil macropores: Principles, controlling factors and consequences for water quality. Eur. J. Soil Sci. 58:523–546. doi:10.1111/j.1365-2389.2007.00915.x

Klaus, J., E. Zehe, M. Elsner, C. Külls, and J.J. McDonnell. 2013. Macropore flow of old water revisited: Experimental insights from a tile-drained hillslope. Hydrol. Earth Syst. Sci. 17:103–118. doi:10.5194/hess-17-103-2013

Knap, K.M., and W.F. Mildner. 1978. Streambank erosion in the Great Lakes basin: Joint summary technical report. International Joint Commission Reference on Pollution from Land Use Activities Reference Group (IJC-PLUARG) technical report. Great Lakes Reg. Office, Windsor, ON.

La Financière Agricole du Québec. 2009. Farm plans and crops 2008 data base. La Financière Agric. Québec. https://www.fadq.qc.ca/documents/donnees/base-de-donnees-des-parcelles-et-productions-agricoles-declarees/ (accessed 31 Oct. 2018).

Macrae, M.L., M.C. English, S.L. Schiff, and M. Stone. 2007. Intra-annual variability in the contribution of tile drains to basin discharge and phosphorus export in a first-order agricultural catchment. Agric. Water Manage. 92:171–182. doi:10.1016/j.agwat.2007.05.015

Matsubayashi, U., G.T. Velasquez, and F. Takagi. 1993. Hydrograph separation and flow analysis by specific electrical conductance of water. J. Hydrol. 152:179–199. doi:10.1016/0022-1694(93)90145-Y

Michaud, A.R., J. Deslandes, and J. Desjardins. 2009a. Réseau d'actions concertées en bassins versants agricoles. Final Proj. Rep. Inst. Rech. Dév. Agroenvironnement, Fonds d'Action Québecois Dév. Durable, Quebec City, QC. https://www.agrireseau.net/agroenvironnement/documents/Rapport%20final.pdf (accessed 31 Oct. 2018).

Michaud, A., J. Deslandes, G. Gagné, L. Grenon, and K. Vézina. 2009b. Gestion raisonnée et intégrée des sols et de l'eau (GRISE). Final Proj. Rep. Inst. Rech. Dév. Agroenvironnement, Adv. Canadian Agric. Agri-Food, Sherbrooke Univ., Cons. Dév. Agric. Québec, Quebec City, QC. https://www.agrireseau.net/agroenvironnement/documents/1_GRISE_2009.pdf (accessed 31 Oct. 2018).

Michaud, A.R., N.-R. Rocha Medrano, R. Lagacé, and A. Drouin. 2014. Développement et validation de méthodes de prédiction du ruissellement et des débits de pointe en support à l'aménagement hydro-agricole. Rapport final présenté au CDAQ dans le cadre du PCAA. Inst. Rech. Dév. Agroenvironnement, Quebec City, QC. https://www.irda.qc.ca/assets/documents/Publications/documents/michaud-et-al-2014_rapport_prediction_ruissellement_ouvrages_hydro-agricoles.pdf (accessed 31 Oct. 2018).

Moriasi, D.N., J.G. Arnold, M.W. Van Liew, R.L. Bingner, R.D. Harmel, and T.L. Veith. 2007. Model evaluation guidelines for systematic quantification of accuracy in watershed simulations. Trans. ASABE 50:885–900. doi:10.13031/2013.23153

Murphy, J., and J.P. Riley. 1962. A modified single solution for the determination of phosphate in natural waters. Anal. Chim. Acta 27:31–36. doi:10.1016/S0003-2670(00)88444-5

Pilgrim, D.H., D.D. Huff, and T.D. Steele. 1979. Use of specific conductance and contact time relations for separating flow components in storm runoff. Water Resour. Res. 15:329–339. doi:10.1029/WR015i002p00329

Poirier, S.C., J.K. Whalen, and A.R. Michaud. 2012. Bioavailable phosphorus in fine-sized sediments transported from agricultural fields. Soil Sci. Soc. Am. J. 76:258–267. doi:10.2136/sssaj2010.0441

SAS Institute. 2008. JMP user guide. SAS version 8.0. SAS Inst., Cary, NC.

Sharpley, A.N., W.W. Troeger, and S.J. Smith. 1991. The measurement of bioavailable phosphorus in agriculture runoff. J. Environ. Qual. 20:235–238. doi:10.2134/jeq1991.00472425002000010037x

Smith, V.H., and D.W. Schindler. 2009. Eutrophication science: Where do we go from here? Trends Ecol. Evol. 24:201–207. doi:10.1016/j.tree.2008.11.009

Stamm, C., H. Flühler, R. Gächter, J. Leuenberger, and H. Wunderli. 1998. Preferential transport of phosphorus in drained grassland soils. J. Environ. Qual. 27:515–522. doi:10.2134/jeq1998.00472425002700030006x

Steenhuis, T.S., J. Boll, G. Shalit, J.S. Selker, and I.A. Merwin. 1994. A simple equation for predicting preferential flow solute concentrations. J. Environ. Qual. 23:1058–1064. doi:10.2134/jeq1994.00472425002300050030x

Vidon, P., and P.E. Cuadra. 2010. Impact of precipitation characteristics on soil hydrology in tile-drained landscapes. Hydrol. Processes 24:1821–1833. doi:10.1002/hyp.7627

Vidon, P., and P.E. Cuadra. 2011. Phosphorus dynamics in tile-drain flow during storms in the US Midwest. Agric. Water Manage. 98:532–540. doi:10.1016/j.agwat.2010.09.010

Walling, D.E., and B.W. Webb. 1980. The spatial dimension in the interpretation of stream solute behaviour. J. Hydrol. 47:129–149. doi:10.1016/0022-1694(80)90052-9

Weiler, M., and F. Naef. 2003. An experimental tracer study of the role of macropores in infiltration in grassland soils. Hydrol. Processes 17:477–493. doi:10.1002/hyp.1136

Williams, M.R., K.W. King, W. Ford, A.R. Buda, and C.D. Kennedy. 2016. Effect of tillage on macropore flow and phosphorus transport to tile drains. Water Resour. Res. 52:2868–2882. doi:10.1002/2015WR017650